IOP Conf. Series: Journal of Physics: Conf. Series **1194** (2019) 012025 doi:10.1088/1742-6596/1194/1/012025

Partial coherent states in graphene

E Díaz-Bautista, J Negro and L M Nieto

Department of Theoretical Physics, Atomic Physics and Optics, University of Valladolid, 47011 Valladolid, Spain

E-mail: ediaz@fis.cinvestav.mx, jnegro@fta.uva.es, luismiguel.nieto.calzada@uva.es

Abstract. We employ a symmetric gauge to describe the interaction of electrons in graphene with a magnetic field which is orthogonal to the layer surface and to build the so-called partial and bidimensional coherent states for this system in the Barut-Girardello sense. We also evaluate the corresponding probability and current densities as well as the mean energy value.

1. Introduction

In 1925 Fock [1] solved the physical problem of a spinless particule moving in the xy-plane under the action of a uniform magnetic field $\vec{B}$ directed along z-axis and an oscillator-like potential $V(x,y)$ employing the so-called symmetric gauge [2,3],

$$\vec{A} = \frac{1}{2}\,\vec{B}\times\vec{r} = \frac{B_0}{2}(-y,x,0), \quad \vec{B} = \nabla\times\vec{A} = B_0\hat{k}. \tag{1}$$

Since then, the motion of a charged particle in a magnetic field became one of the most studied quantum systems. In particular, Man'ko and Malkin [4] were able to build the simplest coherent states for this system as 2-dimensional generalizations of the Glauber ones [5], taking as starting point the results obtained by Landau [6].

On the other hand, graphene is a material that consists in a sheet of carbon atoms arranged on a honeycomb lattice [7–9], in which the dynamics of the electrons close to Dirac points is described by the (2+1) dimensional massless Dirac-like equation with an effective velocity $v_F = c/300$, what results in many relativistic phenomena [7, 9–13]. The interaction of electrons in graphene and magnetic fields has attracted interest in many physics branches [14–23] with the purpose of controlling or confining such particles for the design of electronic devices. Thus, one can try to apply the coherent states formalism in this system considering e.g. homogeneous perpendicular magnetic fields. In [24] coherent states with a translational symmetry along y direction have been constructed assuming the Landau gauge $\vec{A} = B_0 x\hat{j}$, and the time-independent Dirac-Weyl (DW) equation

$$H_{DW}\Psi(x,y) = v_F\,\vec{\sigma}\cdot\left(\vec{p}+\frac{e}{c}\vec{A}\right)\Psi(x,y) = E\Psi(x,y), \tag{2}$$

where $\vec{\sigma} = (\sigma_x,\sigma_y,\sigma_z)$ are the Pauli matrices and $\Psi(x,y)$ are wave functions of two components. Our purpose here is to look for generalizations of those quantum states that preserve the rotational invariance through a symmetric gauge for describing the electron dynamics in graphene.

This work is organized as follows. In Sect. 2, Dirac-Weyl equation is solved for a symmetric gauge and the associated algebraic structure is discussed. In Sect. 3, spinorial families of partial coherent states are obtained as eigenstates of two independent generalized annihilation operators, $\mathbb{A}^-$ and $\mathbb{B}^-$. Also, the corresponding probability and current densities and the mean energy are evaluated. In Sect. 4, bidimensional coherent states for graphene are presented as common eigenstates of both operators $\mathbb{A}^-$ and $\mathbb{B}^-$. Our conclusions are presented in Sect. 5.

2. Dirac-Weyl Hamiltonian

By substituting the symmetric gauge (1) in Eq. (2), we obtain

$$H_{DW}\Psi(x,y) = v_F\left(\sigma_x\left[p_x - \frac{eB_0}{2c}y\right] + \sigma_y\left[p_y + \frac{eB_0}{2c}x\right]\right)\Psi(x,y) = E\Psi(x,y), \tag{3}$$

which can be expressed as

$$H_{DW}\Psi(x,y) = \sqrt{\omega}\hbar\, v_F\begin{bmatrix} 0 & -iA^- \\ iA^+ & 0 \end{bmatrix}\Psi(x,y) = E\Psi(x,y), \quad \Psi(x,y) = \begin{pmatrix} \psi_1(x,y) \\ i\psi_2(x,y) \end{pmatrix},$$

by defining the first order differential operators

$$A^{\pm} = \mp\frac{i}{\sqrt{\omega}\hbar}\left[\left(p_x - \frac{\omega\hbar}{4}y\right) \mp i\left(p_y + \frac{\omega\hbar}{4}x\right)\right],$$

where $\omega = 2eB_0/c\hbar$ is the cyclotron frecuency. The eigenvalue equation (3) encodes two coupled equations:

$$A^-\psi_2(x,y) = \epsilon\psi_1(x,y), \quad A^+\psi_1(x,y) = \epsilon\psi_2(x,y), \quad \epsilon = \frac{E}{\sqrt{\omega}\hbar\, v_F}.$$

which give place to the following equations for each pseudo-spinor component:

$$\mathcal{H}^+\psi_2(x,y) = A^+A^-\psi_2(x,y) = \epsilon^2\psi_2(x,y),$$
$$\mathcal{H}^-\psi_1(x,y) = A^-A^+\psi_1(x,y) = \epsilon^2\psi_1(x,y).$$

Since the problem has a geometrical rotational symmetry around z-axis, it is convenient to express the Hamiltonians $\mathcal{H}^{\pm}$ in polar coordinates (ρ,θ). Thus, by introducing the dimensionless variable ξ and the parameter $\mathcal{E}$, defined as follows:

$$\xi = \frac{\sqrt{\omega}}{2}\rho, \quad \mathcal{E} \equiv \epsilon^2 = \frac{E^2}{\omega\hbar^2 v_F^2},$$

the corresponding eiganvalue equations take the form

$$\mathcal{H}^+\psi_2(\xi,\theta) = \frac{1}{4}\left[-\left(\partial_\xi^2 + \frac{1}{\xi}\partial_\xi + \frac{1}{\xi^2}\partial_\theta^2\right) - 2i\partial_\theta + \xi^2 - 2\right]\psi_2(\xi,\theta) = \mathcal{E}_2\psi_2(\xi,\theta),$$
$$\mathcal{H}^-\psi_1(\xi,\theta) = \frac{1}{4}\left[-\left(\partial_\xi^2 + \frac{1}{\xi}\partial_\xi + \frac{1}{\xi^2}\partial_\theta^2\right) - 2i\partial_\theta + \xi^2 + 2\right]\psi_1(\xi,\theta) = \mathcal{E}_1\psi_1(\xi,\theta).$$

This set of differential equations reminds the known Fock-Darwin system [1, 3, 25]. The above relations imply that the eigenvalues of the Hamiltonians $\mathcal{H}^{\pm}$ are related as $\mathcal{E}_{1,n-1} = \mathcal{E}_{2,n} = n$, and therefore the spectrum of the DW equation (3) is

$$E_n = \pm\hbar v_F\sqrt{n\omega}, \quad n = 0, 1, 2, \ldots,$$

where the negative energies correspond to holes in graphene.

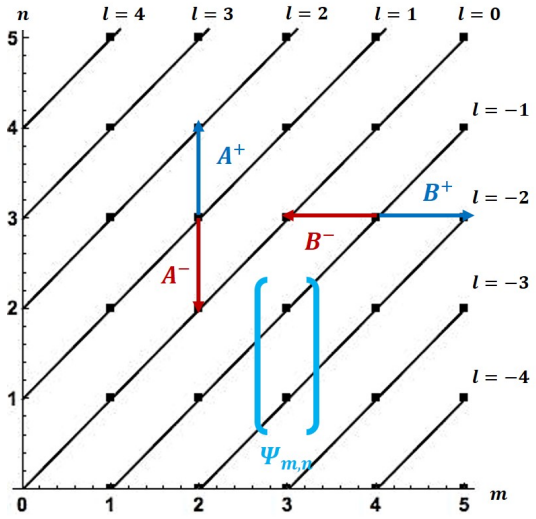

Figure 1: The space of states $\psi_{m,n}$ is represented by coordinates (m, n). Straight lines conect states with the same angular momentum l. The region is divided in two sectors according to the sign of the z-component of the angular momentum: $l \geq 0$ and $l < 0$.

2.1. Algebraic treatment and eigenstates

Both Hamiltonians $\mathcal{H}^{\pm}$ can be factorized in terms of two set of differential operators as [25–27]:

$$\mathcal{H}^{+} = A^{+}A^{-} = B^{+}B^{-} + L_z, \quad \mathcal{H}^{-} = \mathcal{H}^{+} + 1.$$

where, in dimensionless polar coordinates (ξ, θ),

$$A^{+} = \frac{\exp(i\theta)}{2}\left(-\partial_\xi + \frac{-i\partial_\theta}{\xi} + \xi\right), \quad A^{-} = \frac{\exp(-i\theta)}{2}\left(\partial_\xi + \frac{-i\partial_\theta}{\xi} + \xi\right), \tag{4a}$$

$$B^{+} = \frac{\exp(-i\theta)}{2}\left(-\partial_\xi + \frac{i\partial_\theta}{\xi} + \xi\right), \quad B^{-} = \frac{\exp(i\theta)}{2}\left(\partial_\xi + \frac{i\partial_\theta}{\xi} + \xi\right), \tag{4b}$$

$$L_z = N - M = -i\partial_\theta, \qquad N = A^{+}A^{-}, \qquad M = B^{+}B^{-}, \tag{4c}$$

where L_z denotes the component in z-direction of the angular momentum operator. These operators satisfy the following commutation relations

$$[A^{-}, A^{+}] = [B^{-}, B^{+}] = 1, \qquad [A^{\pm}, B^{\pm}] = [A^{\pm}, B^{\mp}] = \mathbf{0}, \tag{5a}$$

$$[L_z, A^{\pm}] = \pm A^{\pm}, \qquad [L_z, B^{\pm}] = \mp B^{\pm}. \tag{5b}$$

Therefore, Eqs. (5a) and (5b) imply that the operators A^{+} and A^{-}, acting on an eigenstate of L_z, increases or decreases, respectively, the eigenvalue of L_z in an unity; the operators $B^{\pm}$ have the contrary effect.

The eigenstates of the Hamiltonians $\mathcal{H}^{\pm}$ are labeled by two positive integer numbers m, n, that are the eigenvalues of the number operators M and N, respectively (see Figure 1):

$$\psi_1(\xi, \theta) \equiv \psi_{m,n-1}(\xi, \theta), \quad \psi_2(\xi, \theta) \equiv \psi_{m,n}(\xi, \theta),$$

while Eq. (4c) implies that the states $\psi_{m,n}$ are also eigenstates of the operator L_z with eigenvalue $l = n - m$. Also, the action of the operators $A^{\pm}$ and $B^{\pm}$ on such states is

$$A^{-}\psi_{m,n} = \sqrt{n}\,\psi_{m,n-1}, \quad A^{+}\psi_{m,n} = \sqrt{n+1}\,\psi_{m,n+1},$$
$$B^{-}\psi_{m,n} = \sqrt{m}\,\psi_{m-1,n}, \quad B^{+}\psi_{m,n} = \sqrt{m+1}\,\psi_{m+1,n}.$$

On the other hand, the normalized eigenfunctions of the Hamiltonian $\mathcal{H}^+$ turn out to be

$$\psi_{m,n}(\rho,\theta)=(-1)^{\min(m,n)}\sqrt{\frac{\omega}{4\pi}\frac{\min(m,n)!}{\max(m,n)!}}\left(\frac{\sqrt{\omega}}{2}\rho\right)^{|n-m|}\exp\left(-\frac{\omega}{8}\rho^2+i(n-m)\theta\right)L^{|n-m|}_{\min(m,n)}\left(\frac{\omega}{4}\rho^2\right), \tag{6}$$

$n,m=0,1,2,\ldots$, while the normalized eigenfunctions of the Hamiltonian $\mathcal{H}^-$ are obtained as $\psi_{m,n-1}=A^-\psi_{m,n}/\sqrt{n}$. These kind of solutions were obtained initially in [1].

Furthermore, we can label as $\Psi^+_{m,n}(x,y)$ the spinorial states whose two scalar components have positive z-component of the angular momentum ($l\geq 0$), and as $\Psi^-_{m,n}(x,y)$ those ones whose two scalar components have negative z-component of the angular momentum ($l<0$), *i.e.*,

$$\Psi^+_{m,n}(x,y)=\frac{1}{\sqrt{2}}\begin{pmatrix}\psi^+_{m,n-1}(x,y)\\ i\psi^+_{m,n}(x,y)\end{pmatrix},\quad \Psi^-_{m,n}(x,y)=\frac{1}{\sqrt{2^{(1-\delta_{0n})}}}\begin{pmatrix}(1-\delta_{0n})\psi^-_{m,n-1}(x,y)\\ i\psi^-_{m,n}(x,y)\end{pmatrix},$$

where $\psi^+_{m,n}(x,y)\equiv\psi^+_{m,n}(\rho,\theta)$ ($\psi^-_{m,n}(x,y)\equiv\psi^-_{m,n}(\rho,\theta)$) identifies the states that belong to the upper (lower) sector in Figure 1, and δ_{mn} denotes the Kronecker delta.

In addition, by defining the total angular momentum operator in z-direction as $\mathbb{J}_z=L_z\otimes\mathbb{I}+\sigma_z/2$, we have that

$$\mathbb{J}_z\Psi_{m,n}(x,y)=\frac{l-1/2}{\sqrt{2^{(1-\delta_{0n})}}}\begin{pmatrix}(1-\delta_{0n})\psi_{m,n-1}(x,y)\\ i\psi_{m,n}(x,y)\end{pmatrix}=j\,\Psi_{m,n}(x,y), \tag{7}$$

i.e., the states $\Psi_{m,n}(x,y)$ are also eigenstates of $\mathbb{J}_z$ with eigenvalue $j\equiv l-1/2$.

3. Partially displaced states

Defining generalized annihilation operators $\mathbb{A}^-$ and $\mathbb{B}^-$ in terms of the scalar ones A^- and B^-, we can build bidimensional coherent states (2D-CS) $\Psi_{\alpha,\beta}(x,y)\equiv\langle x,y|\alpha,\beta\rangle$ such that [4,25,28]:

$$\mathbb{A}^-\Psi_{\alpha,\beta}(x,y)=\alpha\Psi_{\alpha,\beta}(x,y),\quad \mathbb{B}^-\Psi_{\alpha,\beta}(x,y)=\beta\Psi_{\alpha,\beta}(x,y),\quad \alpha,\beta\in\mathbb{C}.$$

Moreover, if one takes specific sums over one of the quantum numbers, n or m, the so-called partial coherent states (PCS) can be obtained [4,28]. In this section, we discuss the construction of all these coherent states for graphene.

3.1. Annihilation operator $\mathbb{B}^-$

Let us consider the operator $\mathbb{B}^-$ defined as

$$\mathbb{B}^-=B^-\otimes\mathbb{I}=\begin{bmatrix}B^- & 0\\ 0 & B^-\end{bmatrix},\quad \mathbb{B}^+=(\mathbb{B}^-)^\dagger\quad\Longrightarrow\quad[\mathbb{B}^-,\mathbb{B}^+]=\mathbb{I}, \tag{8}$$

such that

$$\mathbb{B}^-\Psi^\pm_{m,n}(x,y)=\sqrt{m}\Psi^\pm_{m-1,n}(x,y).$$

A first family of PCS $\Psi^n_\beta(x,y)\equiv\langle x,y|n,\beta\rangle$ is obtained from the eigenvalue equation

$$\mathbb{B}^-\Psi^n_\beta(x,y)=\beta\Psi^n_\beta(x,y),\quad \beta\in\mathbb{C},\quad n=0,1,2,\ldots.$$

The PCS with a well-defined energy $E_n=\sqrt{n\omega}\,\hbar v_F$ turn out to be

$$\Psi^n_\beta(x,y)=\frac{1}{\sqrt{2^{(1-\delta_{0n})}}}\begin{pmatrix}(1-\delta_{0n})\psi^{n-1}_\beta(x,y)\\ i\psi^n_\beta(x,y)\end{pmatrix},\quad n=0,1,2,\ldots, \tag{9}$$

where we have identified two scalar eigenstates ψ_β^n of B^- for each energy level n.

Now, each scalar coherent state in Eq. (9) satisfies one of these equation systems:

$$B^-\psi_\beta^n(x,y) = \beta\psi_\beta^n(x,y), \qquad A^+A^-\psi_\beta^n(x,y) = n\,\psi_\beta^n(x,y), \tag{10a}$$

$$B^-\psi_\beta^{n-1}(x,y) = \beta\psi_\beta^{n-1}(x,y), \qquad A^-A^+\psi_\beta^{n-1}(x,y) = n\,\psi_\beta^{n-1}(x,y). \tag{10b}$$

Therefore, in order to find the solutions ψ_β^n, one should define the complex parameter z as

$$z = \frac{\sqrt{\omega}}{2}\rho\exp(i\theta) = \sqrt{\omega}\left(\frac{x+iy}{2}\right), \tag{11}$$

and the operators $A^\pm$ and $B^\pm$ should be also expressed in terms of z. Thus, after solving the expressions in Eq. (10), the normalized spinorial PCS $\Psi_\beta^n(x,y)$, $n = 0, 1, 2, \ldots$, take the form

$$\Psi_\beta^n(x,y) = \frac{1}{\sqrt{2^{(1-\delta_{0n})}\pi\, n!}}\exp\left(\left[\beta - \frac{z}{2}\right]z^* - \frac{|\beta|^2}{2}\right)\begin{pmatrix}\sqrt{n}(z-\beta)^{n-1}\\ i(z-\beta)^n\end{pmatrix}. \tag{12}$$

As a final comment, let us mention that the coherent states $\Psi_\beta^n(x,y)$ can be also obtained by operating an unitary displacement operator $\mathbb{D}(\beta,\beta^*)$ on the spinorial states $\Psi_{0,n}(x,y)$, *i.e.*,

$$\Psi_\beta^n(x,y) = \mathbb{D}(\beta,\beta^*)\Psi_{0,n}^-(x,y), \quad \mathbb{D}(\beta,\beta^*) = \exp\left(\beta\mathbb{B}^+ - \beta^*\mathbb{B}^-\right). \tag{13}$$

3.1.1. Probability and current densities. From Eq. (13), we can establish that the coherent states $\Psi_\beta^n(x,y)$ are displaced from the origin, similarly to the standard coherent states (SCS) in phase space, being centered at the point

$$(x_0,y_0) = \left(\frac{2|\beta|}{\sqrt{\omega}}\cos(\varphi), \frac{2|\beta|}{\sqrt{\omega}}\sin(\varphi)\right), \quad \beta = |\beta|\exp(i\varphi).$$

Such a translation is generated through the magnetic translational operators that represent, in a classical interpretation, the coordinates of the centre of a circle on xy-plane in which a charged particle moves [29–32]. In complex number notation, the coordinates (x,y) with respect to the origin of such a particle moving in a circular trajectory of radius $\rho' = \sqrt{x'^2+y'^2}$, will be

$$z = \sqrt{\omega}\left(\frac{x+iy}{2}\right) = (|\beta|\cos(\varphi) + \xi'\cos(\theta')) + i(|\beta|\sin(\varphi) + \xi'\sin(\theta')) = \beta + z',$$

where $\xi' = \sqrt{\omega}\rho'/2$ and $z' = \xi'\exp(i\theta')$. Hence, the probability density $\rho_{n,\beta}(x,y)$ and the current densities $j_{n,\hat{n}'\beta}(x',y')$ along the directions of the vectors $\hat{\rho}'$ and $\hat{\theta}'$ in the displaced frame are, respectively (see Figure 2):

$$\rho_{n,\beta}(x,y) = \Psi_\beta^{n\dagger}(x,y)\Psi_\beta^n(x,y) = \frac{1}{2^{(1-\delta_{0n})}\pi\, n!}\exp\left(-|z-\beta|^2\right)|z-\beta|^{2n-2}\left[|z-\beta|^2+n\right],$$

$$j_{n,\hat{n}'\beta}(x',y') = ev_F\Psi_\beta^{n\dagger}(x',y')\,(\vec{\sigma}\cdot\hat{n}')_k\,\Psi_\beta^n(x',y') = \frac{2\,ev_F\sqrt{n}}{2^{(1-\delta_{0n})}\pi\, n!}\exp\left(-|z'|^2\right)\frac{|z'|^{2n}}{\xi'}\Re[i(-i)^k].$$

For $k = 0$ ($k = 1$), last equation gives the flux of probability in the radial (angular) direction. As is expected, the function $j_{n,\hat{\rho}'\beta}(x',y')$ is null for any value of n.

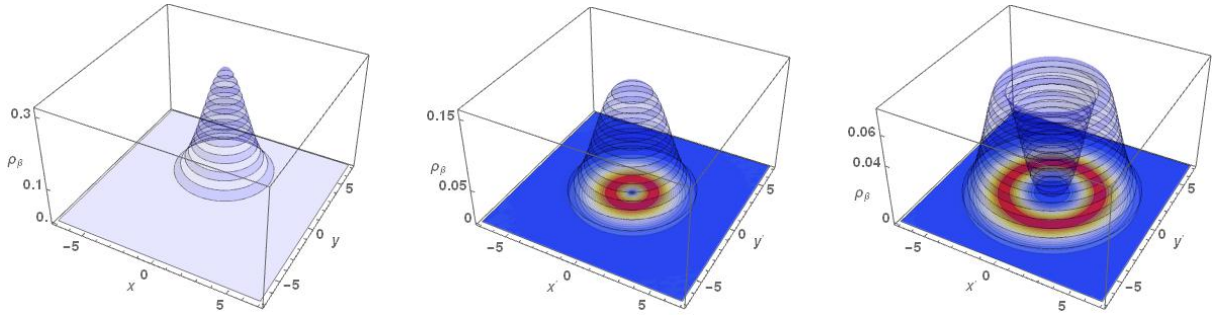

(a) $\rho_{n,\beta}(x,y)$ for $n=0$ and $\beta=\exp(i\pi/2)$

(b) $\rho_{n,\beta}(x',y')$ and $j_{n,\hat{\theta}'\beta}(x',y')$ with $\beta=1$ and $n=1$

(c) $\rho_{n,\beta}(x',y')$ and $j_{n,\hat{\theta}'\beta}(x',y')$ with $\beta=1$ and $n=3$

Figure 2: For PCS $\Psi^n_\beta(x,y)$, the probability density $\rho_{n,\beta}(x,y)$ (3D) as well the angular current density $j_{n,\hat{\theta}'\beta}(x',y')$ (2D) are shown for different values of n, for $B_0=1/2$ and $\omega=1$.

3.2. Annihilation operator $\mathbb{A}^-$

Now, let us consider the operator $\mathbb{A}^-$ defined as

$$\mathbb{A}^- = \frac{1}{\sqrt{2}}\begin{bmatrix} \frac{\sqrt{N+2}}{\sqrt{N+1}}A^- & \frac{1}{\sqrt{N+1}}(A^-)^2 \\ -\sqrt{N+1} & A^- \end{bmatrix}, \quad \mathbb{A}^+ = (\mathbb{A}^-)^\dagger \quad \Longrightarrow \quad [\mathbb{A}^-,\mathbb{A}^+] = \mathbb{I}, \tag{14}$$

such that

$$\mathbb{A}^-\Psi_{m,n}(x,y) = \frac{\sqrt{n}}{\sqrt{2^{\delta_{1n}}}}\exp(i\pi/4)\Psi_{m,n-1}, \quad n=0,1,2,\ldots.$$

A second family of PCS $\Psi^m_\alpha(x,y)\equiv\langle x,y|\alpha,m\rangle$ is obtained from the eigenvalue equation

$$\mathbb{A}^-\Psi^m_\alpha(x,y) = \alpha\Psi^m_\alpha(x,y), \quad \alpha\in\mathbb{C}, \quad m=0,1,2,\ldots. \tag{15}$$

By applying Eq. (15) and taking $\tilde{\alpha}=\alpha\exp(-i\pi/4)$, the corresponding PCS take the form

$$\Psi^m_\alpha(x,y) = \left[2\exp(|\tilde{\alpha}|^2)-1\right]^{-1/2}\left[\Psi^-_{m,0}(x,y) + (1-\delta_{0m})\sum_{n=1}^{m}\frac{\sqrt{2}\tilde{\alpha}^n}{\sqrt{n!}}\Psi^-_{m,n}(x,y) + \sum_{n=m+1}^{\infty}\frac{\sqrt{2}\tilde{\alpha}^n}{\sqrt{n!}}\Psi^+_{m,n}(x,y)\right]. \tag{16}$$

3.2.1. Probability and current densities and mean energy. Using again the complex parameter z in Eq. (11), the densities $\rho_{m,\alpha}(x,y)$ and $j_{m,\hat{n}\alpha}(x,y)$, and the mean energy $\langle H_{DW}\rangle_\alpha$ are

$$\begin{aligned}
&\rho_{m,\alpha}(x,y) = \rho_{m,\alpha}(\rho,\theta) = \Psi^{m\dagger}_\alpha(x,y)\Psi^m_\alpha(x,y)\\
&= \left[2\exp(|\tilde{\alpha}|^2)-1\right]^{-1}\left[g^2_m(\rho) + \left|\sum_{n=m+1}^{\infty}\frac{(\tilde{\alpha}z)^n}{n!}L^{n-m}_m\left(\frac{\omega}{4}\rho^2\right)f_m(\rho)\right|^2\right.\\
&+\left|\sum_{n=m+1}^{\infty}\frac{(\tilde{\alpha}z)^n}{n!}\frac{\sqrt{n}}{z}L^{n-m-1}_m\left(\frac{\omega}{4}\rho^2\right)f_m(\rho)\right|^2 + 2\Re\left[\sum_{n=m+1}^{\infty}\frac{(\tilde{\alpha}z)^n}{n!}f_m(\rho)g_m(\rho)L^{n-m}_m(\rho^2)\right]\\
&+(1-\delta_{0m})\left(\left|\sum_{n=1}^{m}\left(-\frac{\tilde{\alpha}}{z^*}\right)^n L^{m-n}_n\left(\frac{\omega}{4}\rho^2\right)g_m(\rho)\right|^2 + \left|\sum_{n=1}^{m}\left(-\frac{\tilde{\alpha}}{z^*}\right)^n\frac{z^*}{\sqrt{n}}L^{m-n+1}_{n-1}\left(\frac{\omega}{4}\rho^2\right)g_m(\rho)\right|^2\right.\\
&\left.+2\Re\left[\sum_{n=1}^{m}\left(-\frac{\tilde{\alpha}}{z^*}\right)^n L^{m-n}_n\left(\frac{\omega}{4}\rho^2\right)g^2_m(\rho) + \left(\sum_{n'=1}^{m}\left(-\frac{\tilde{\alpha}^*}{z}\right)^{n'} L^{m-n'}_{n'}\left(\frac{\omega}{4}\rho^2\right)g_m(\rho)\right)\times\right.
\end{aligned}$$

$$\times \left(\sum_{n=m+1}^{\infty} \frac{(\tilde{\alpha}z)^n}{n!} L_m^{n-m}\left(\frac{\omega}{4}\rho^2\right) f_m(\rho) \right) - \left(\sum_{n'=1}^{m} \left(-\frac{\tilde{\alpha}^*}{z}\right)^{n'} \frac{1}{\sqrt{n'}} L_{n'-1}^{m-n'+1}\left(\frac{\omega}{4}\rho^2\right) g_m(\rho) \right) \times$$
$$\times \left(\sum_{n=m+1}^{\infty} \frac{(\tilde{\alpha}z)^n}{n!} \sqrt{n} L_m^{n-m-1}\left(\frac{\omega}{4}\rho^2\right) f_m(\rho) \right) \Bigg] \Bigg) \Bigg], \tag{17a}$$

$$j_{m,\hat{n}\alpha}(x,y) = j_{m,\hat{n}\alpha}(\rho,\theta) = ev_F \Psi_\alpha^{m\dagger}(x,y) \left(\vec{\sigma}\cdot\hat{n}\right)_k \Psi_\alpha^m(x,y)$$
$$= \frac{2ev_F}{2\exp(|\tilde{\alpha}|^2)-1} \Re\Bigg[i(-i)^k e^{-i\theta} \Bigg\{ \sum_{n=m+1}^{\infty} \frac{(\tilde{\alpha}^* z^*)^n}{n!} \frac{\sqrt{n}}{z^*} L_m^{n-m-1}\left(\frac{\omega}{4}\rho^2\right) f_m(\rho) g_m(\rho)$$
$$+ \left(\sum_{n'=m+1}^{\infty} \frac{(\tilde{\alpha}z)^{n'}}{n'!} L_m^{n'-m}\left(\frac{\omega}{4}\rho^2\right) f_m(\rho) \right) \left(\sum_{n=m+1}^{\infty} \frac{(\tilde{\alpha}^* z^*)^n}{n!} \frac{\sqrt{n}}{z^*} L_m^{n-m-1}\left(\frac{\omega}{4}\rho^2\right) f_m(\rho) \right)$$
$$- (1-\delta_{0m}) \left(\sum_{n=1}^{m} \left(-\frac{\tilde{\alpha}^*}{z}\right)^n \frac{z}{\sqrt{n}} L_{n-1}^{m-n+1}\left(\frac{\omega}{4}\rho^2\right) g_m^2(\rho) \right.$$
$$+ \left(\sum_{n'=1}^{m} \left(-\frac{\tilde{\alpha}}{z^*}\right)^{n'} L_{n'}^{m-n'}\left(\frac{\omega}{4}\rho^2\right) g_m(\rho) \right) \left(\sum_{n=1}^{m} \left(-\frac{\tilde{\alpha}^*}{z}\right)^n \frac{z}{\sqrt{n}} L_{n-1}^{m-n+1}\left(\frac{\omega}{4}\rho^2\right) g_m(\rho) \right)$$
$$- \left(\sum_{n'=1}^{m} \left(-\frac{\tilde{\alpha}}{z^*}\right)^{n'} L_{n'}^{m-n'}\left(\frac{\omega}{4}\rho^2\right) g_m(\rho) \right) \left(\sum_{n=m+1}^{\infty} \frac{(\tilde{\alpha}^* z^*)^n}{n!} \frac{\sqrt{n}}{z^*} L_m^{n-m-1}\left(\frac{\omega}{4}\rho^2\right) f_m(\rho) \right)$$
$$+ \left(\sum_{n'=m+1}^{\infty} \frac{(\tilde{\alpha}z)^{n'}}{n'!} L_m^{n'-m}\left(\frac{\omega}{4}\rho^2\right) f_m(\rho) \right) \left(\sum_{n=1}^{m} \left(-\frac{\tilde{\alpha}^*}{z}\right)^n \frac{z}{\sqrt{n}} L_{n-1}^{m-n+1}\left(\frac{\omega}{4}\rho^2\right) g_m(\rho) \right) \Bigg) \Bigg\} \Bigg], \tag{17b}$$

$$\langle H_{DW}\rangle_\alpha = \frac{2\sqrt{\omega}\hbar v_F}{2\exp\left(|\tilde{\alpha}|^2\right)-1} \sum_{n=0}^{\infty} \frac{|\tilde{\alpha}|^{2n}}{n!}\sqrt{n}, \tag{17c}$$

where

$$f_m(\rho) = \sqrt{\frac{\omega\, m!}{4\pi}} \left(-\frac{2}{\sqrt{\omega}}\rho^{-1}\right)^m \exp\left(-\frac{\omega}{8}\rho^2\right), \quad g_m(\rho) = \sqrt{\frac{\omega}{4\pi\, m!}} \left(\frac{\sqrt{\omega}}{2}\rho\right)^m \exp\left(-\frac{\omega}{8}\rho^2\right).$$

For $k=0$ ($k=1$), Eq. (17b) gives the flux of probability in the radial (angular) direction. Both functions are not null for any value of m (see Figure 3). Meanwhile, the mean energy function (17c) is shown in Figure 4.

4. Bidimensional coherent states

Finally, 2D-CS built in [4] can be also obtained for graphene as [28]:

$$\Psi_{\alpha,\beta}(x,y) = \mathcal{N}\sum_{n=0}^{\infty} c_n \Psi_\beta^n(x,y) = \mathcal{N}\sum_{m=0}^{\infty} d_m \Psi_\alpha^m(x,y) = \mathcal{N}\Psi_\alpha^m(x,y)\Psi_\beta^n(x,y),$$

where $\mathcal{N}$ is a normalization constant. Hence, employing the coherent states shown in Eqs. (12) and (16), we obtain the following expressions for 2D-CS, as well their corresponding probability and current densities (see Figure 5):

$$\Psi_{\alpha,\beta}(x,y) = \frac{\exp\left(\left[\beta-\frac{z}{2}\right]z^* - \frac{|\beta|^2}{2}\right)}{\sqrt{\pi(2\exp(|\tilde{\alpha}|^2)-1)}} \sum_{n=0}^{\infty} \frac{\tilde{\alpha}^n}{n!} \begin{pmatrix} \sqrt{n}(z-\beta)^{n-1} \\ i(z-\beta)^n \end{pmatrix}, \tag{18a}$$

$$\rho_{\alpha,\beta}(x,y) = \frac{\exp\left(-|z-\beta|^2\right)}{\pi(2\exp(|\tilde{\alpha}|^2)-1)} \left[1 + \left| \sum_{n=1}^{\infty} \frac{[\tilde{\alpha}(z-\beta)]^n}{n!} \right|^2 + \left| \sum_{n=1}^{\infty} \frac{[\tilde{\alpha}(z-\beta)]^n \sqrt{n}}{n!(z-\beta)} \right|^2 + 2\Re\left[\sum_{n=1}^{\infty} \frac{[\tilde{\alpha}(z-\beta)]^n}{n!} \right] \right], \tag{18b}$$

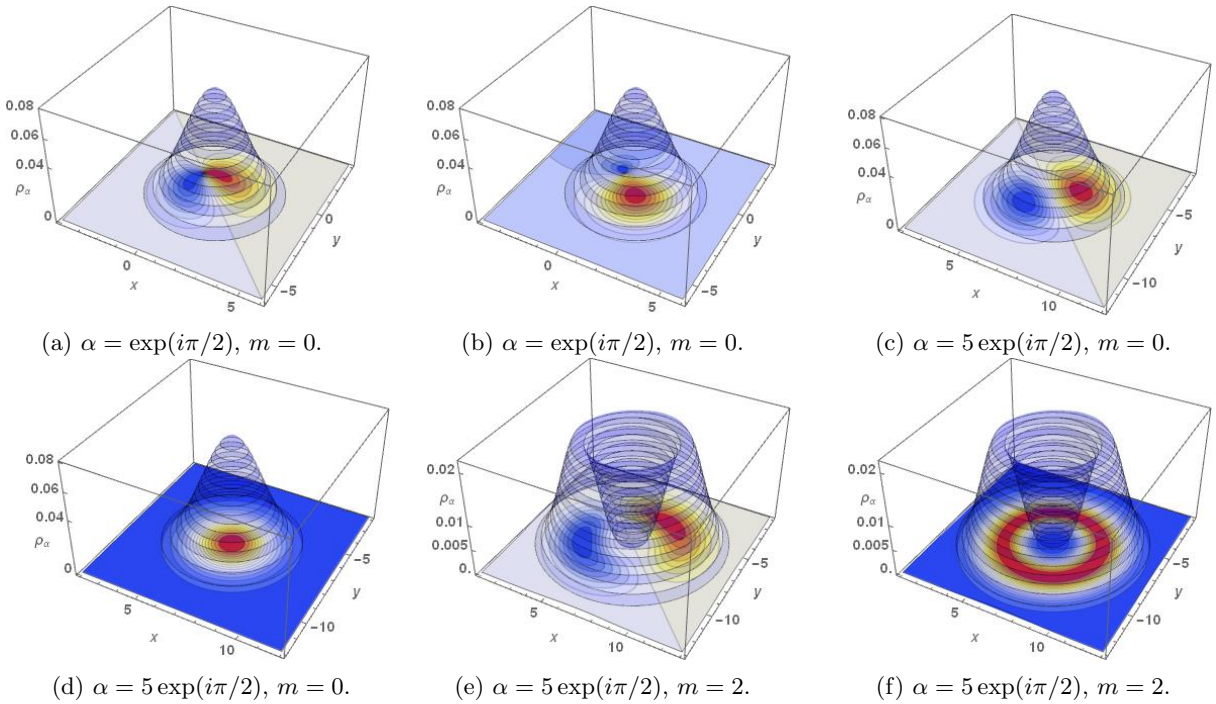

(a) $\alpha = \exp(i\pi/2)$, $m = 0$. (b) $\alpha = \exp(i\pi/2)$, $m = 0$. (c) $\alpha = 5\exp(i\pi/2)$, $m = 0$.

(d) $\alpha = 5\exp(i\pi/2)$, $m = 0$. (e) $\alpha = 5\exp(i\pi/2)$, $m = 2$. (f) $\alpha = 5\exp(i\pi/2)$, $m = 2$.

Figure 3: For PCS $\Psi^m_\alpha(x, y)$, the probability density $\rho_{m,\alpha}(x, y)$ (3D), the radial current density $j_{m,\hat{\rho}\alpha}(x, y)$ (2D, a, c, e) and the angular current density $j_{m,\hat{\theta}\alpha}(x, y)$ (2D, b, d, f) are shown for some values of α and m. In all the cases $B_0 = 1/2$ and $\omega = 1$.

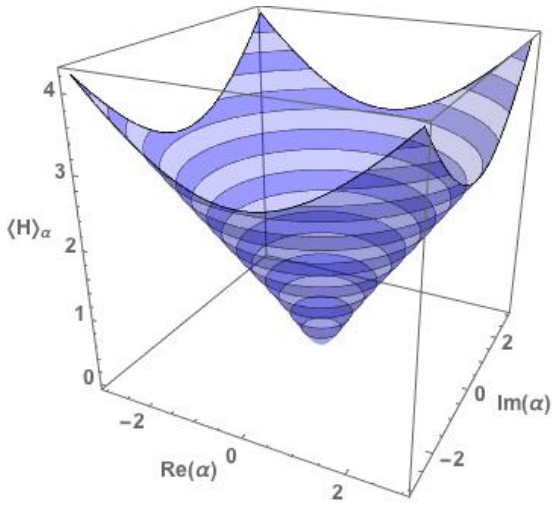

Figure 4: $\langle H\rangle_\alpha$ as a continous function of α for the PCS $\Psi^m_\alpha(x, y)$, with $B_0 = 1/2$ and $\omega = 1$.

$$j_{\alpha,\beta,\hat{n}}(x, y) = \frac{2ev_F \exp\left(-|z-\beta|^2\right)}{\pi(2\exp(|\tilde{\alpha}|^2) - 1)} \Re\left[i(-i)^k e^{-i\theta} \left(\sum_{n'=0}^{\infty} \frac{[\tilde{\alpha}(z-\beta)]^{n'}}{n'!} \right) \left(\sum_{n=0}^{\infty} \frac{[\tilde{\alpha}^*(z^*-\beta^*)]^n \sqrt{n}}{n!(z^*-\beta^*)} \right) \right]. \quad (18c)$$

The expression for the mean energy $\langle H_{DW}\rangle_\alpha$ for these states is the same than those ones in Eq. (16) due to the coherent states $\Psi^n_\beta(x, y)$ are actually stationay states (see Figure 4).

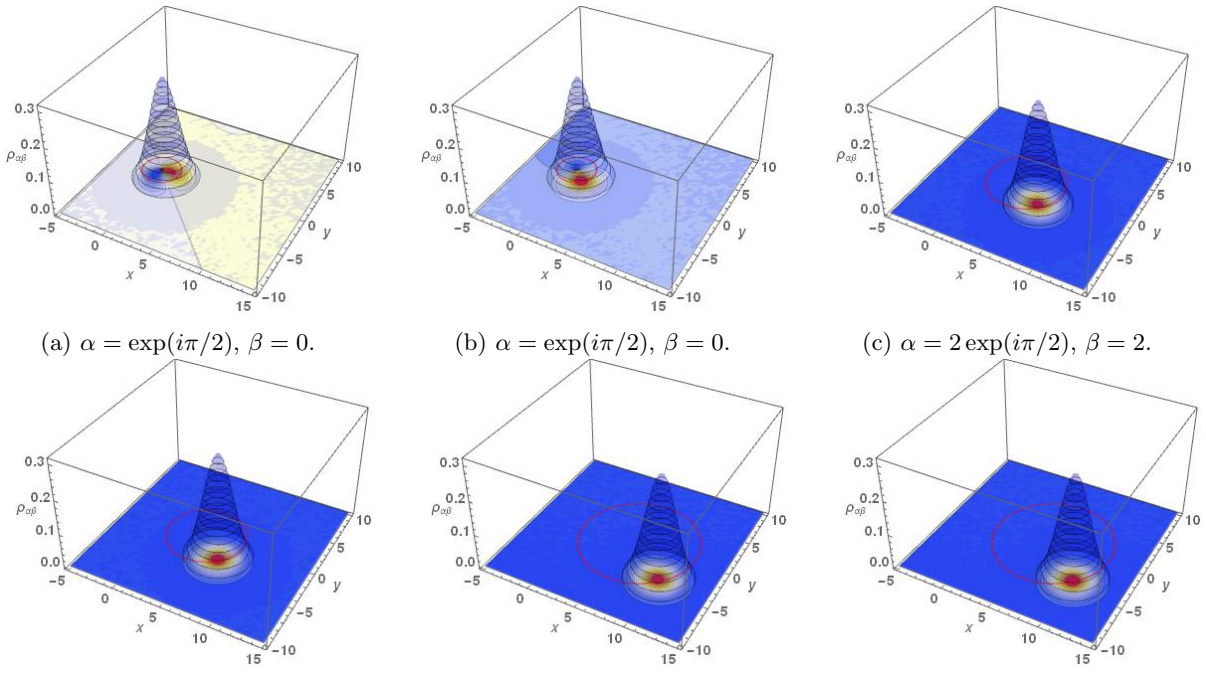

(a) $\alpha = \exp(i\pi/2)$, $\beta = 0$. (b) $\alpha = \exp(i\pi/2)$, $\beta = 0$. (c) $\alpha = 2\exp(i\pi/2)$, $\beta = 2$.

(d) $\alpha = 2\exp(i\pi/2)$, $\beta = 2$. (e) $\alpha = 3\exp(i\pi/2)$, $\beta = 3$. (f) $\alpha = 3\exp(i\pi/2)$, $\beta = 3$.

Figure 5: For 2D-CS $\Psi_{\alpha,\beta}(x,y)$, the probability density $\rho_{\alpha,\beta}(x,y)$ (3D) and radial current density $j_{\alpha,\beta,\hat{\rho}}(x,y)$ (2D, a, c, e), as well the angular current density $j_{\alpha,\beta,\hat{\theta}}(x,y)$ (2D, b, d, f) are shown for some values of α and β. In all the cases $B_0 = 1/2$ and $\omega = 1$. Red lines on xy-plane correspond to the classical trajectory of a charged particle in a magnetic field: the coordinates of the center of the circle are determined by β while α gives the coordinates in which the maximum probability amplitude can be found respect to that point.

5. Conclusions

In this work, we have followed the ideas of Malkin and Man'ko [4] to obtain the simplest coherent states for electrons in graphene interacting with a magnetic field through a symmetric gauge, in order to describe the dynamics of such particles close to Dirac points.

For the gauge considered, DW solutions have axial symmetry (Eq. (6)) and infinite degeneracy due to the existance of rotational symmetry, $[\mathcal{H}^{\pm}, L_z] = \mathbf{0}$. Two sets of scalar ladder operators are identified and whith them, we can define two generalized annihilation operators $\mathbb{A}^-$ and $\mathbb{B}^-$ (Eqs. (8) and (14)) with which we can build their associated coherent states. Hence, three different kinds of coherent states $\Psi^n_\beta(x,y)$, $\Psi^m_\alpha(x,y)$ and $\Psi_{\alpha,\beta}(x,y)$ with non-definite angular momentum are obtained. For the coherent states in Eqs. (16) and (18a), there is a flux of probability in both radial and angular directions that, we assume, it is due to the contribution of the wave functions of both sublattices in the unit cell of graphene (Figures 3, 5). Meanwhile, for the states in Eq. (12), there is only flux of probability in angular direction with axial symmetry because these ones are actually stationary states that have been displaced on xy-plane (Figure 2).

On the other hand, both families of PCS $\Psi^n_\beta(x,y)$ and $\Psi^m_\alpha(x,y)$ posses a Gaussian probability distribution only for $n = 0$ and $m = 0$, respectively (Figures 2, 3), while 2D-CS $\Psi_{\alpha,\beta}(x,y)$ have a stable Gaussian-like probability distribution regardless the value of α and β, as happens with SCS in phase space. Similar to what is observed for the bidimensional coherent states obtained by Malkin and Man'ko, in a semi-classical interpretation, the eigenvalue β determines

the coordinates of the center of the circle while α is related with the coordinates of the charged particle rotating around such center (see Figure 5). This allows us to conclude that these last coherent states are the simplest ones that can be obtained for electrons in graphene interacting with an external constant magnetic field for a symmetric gauge [4]. In addition, the behavior of the mean energy function suggests the possibility of using both states $\Psi_\alpha^m(x,y)$ and $\Psi_{\alpha,\beta}(x,y)$ in semi-classical treatments (Figure 4).

Finally, it is important to remark that, as has been discussed in [33–35], it is possible to construct coherent states that are also eigenstates of the total angular momentum operator in z-direction (Eq. (7)) through ladder operators $\mathcal{K}^- = \mathbb{A}^-\mathbb{B}^-$, $\mathcal{K}^+ = (\mathcal{K}^-)^\dagger$ that, together with the operator $2\mathcal{K}_0 = [\mathcal{K}^-, \mathcal{K}^+]$, are generators of $su(1,1)$ algebra. This work is in progress.

Acknowledgments

This work has been supported in part by the Spanish Junta de Castilla y León (Projects VA137G18 and BU229P18) and MINECO (Project MTM2014-57129-C2-1-P). EDB also acknowledges the support of Conacyt and the warm hospitality at Department of Theoretical Physics of the University of Valladolid, as well his family moral support, specially of Act. J. Manuel Zapata L.

References

[1] Fock V 1928 *Z. Phys.* **47** 446
[2] Page L 1930 *Phys. Rev.* **36** 444
[3] Darwin C G 1931 *Math. Proc. Cambridge Phil. Soc.* **27** 86
[4] Mankin I A and Man'ko V I 1968 *Sov. Phys. JETP* **55** 1014; 1969 *Sov. Phys. JETP* **28** 527
[5] Glauber R J 1963 *Phys. Rev.* **131** 2766
[6] Landau L 1930 *Z. Phys.* **64** 629
[7] Novoselov K S, Geim A K, Morozov S M, Zhang Y, Dubonos S V, Grigorieva I V and Firsov A A 2004 *Science* **306** 666
[8] Zheng Y, Tan J W, Stormer H L and Kim P 2005 *Nature* **438** 201
[9] Castro Neto A H, Guinea F, Peres N M, Novoselov K S and Geim A K 2009 *Rev. Mod. Phys.* **81** 109
[10] Katsnelson M I, Novoselov K S and Geim A K 2006 *Nature Phys.* **2** 620
[11] Schakel A M J 1991 *Phys. Rev.* D **43** 1428
[12] Katsnelson M I 2006 *Eur. Phys. J.* B **51** 157
[13] Rusin T M and Zawadzki W 2007 *Phys. Rev.* B **76** 195439; 2008 *Phys. Rev.* B **78** 125419
[14] De Martino A, Dell'Anna L and Egger R 2007 *Phys. Rev. Lett.* **98** 066802
[15] Dell'Anna L and De Martino A 2009 *Phys. Rev.* B **79** 045420
[16] Giavaras G, Maksym P A and Roy M 2009 *J. Phys: Condens. Matter.* **21** 102201
[17] Kuru Ş, Negro J and Nieto L M 2009 *J. Phys.: Condens. Matter* **21** 455305
[18] Midya B and Fernández D J 2014 *J. Phys.* A **47** 035304
[19] Ramezani Masir M, Vasilopoulos P and Peeters F M J 2011 *Phys: Condens. Matter.* **23** 315301
[20] Downing C A and Portnoi M E 2016 *Phys. Rev.* B **94** 165407; 2016 *Phys. Rev.* B **94** 045430
[21] Eshghi M, Mehraban H and Ahmadi Azar I 2017 *Physica* E **94** 106
[22] Roy P, Ghosh T K and Bhattacharya K 2012 *J. Phys. Condens. Matter* **24** 055301
[23] Dai-Nam L, Van-Hoang L and Pinaky R 2017 *Physica* E **96** 17
[24] Díaz-Bautista E and Fernández D J 2017 *Eur. Phys. J.* Plus **132** 499
[25] Drigho-Filho E, Kuru Ş, Negro J and Nieto L M 2017 *Ann. Phys.* **383** 101
[26] Fernández D J 1996 *Ann. Phys.* **252** 386
[27] Kikoin K, Kiselev M and Avishai Y 2012 *Dynamical Symmetries for Nanostructures* (Vienna: Springer)
[28] Dodonov V V 2018 *Coherent States and Their Applications: A Contemporary Panorama* (New York: Springer Proceedings in Physics) **205** 311
[29] Brown E 1964 *Phys. Rev.* **133** A1038
[30] Zack J 1964 *Phys. Rev.* **134** A1602
[31] Laughlin R B 1983 *Phys. Rev.* B **27** 3383
[32] Kowalski K and Rembieliński J 2005 *J. Phys. A: Math. Gen.* **38** 8247
[33] Novaes M and Gazeau J P 2003 *J. Phys. A: Math. Gen.* **36** 199-212
[34] Dehghani A, Fakhri H and Mojaveri B 2012 *J. Math. Phys.* **53** 123527
[35] Dehghani A and Mojaveri B 2013 *Eur. Phys. J.* D **67** 264